
Masters Theses

Student Theses and Dissertations

1968

Infrared related solid state studies

Donald George Rathbun

Follow this and additional works at: https://scholarsmine.mst.edu/masters_theses



Part of the [Physics Commons](#)

Department:

Recommended Citation

Rathbun, Donald George, "Infrared related solid state studies" (1968). *Masters Theses*. 5252.
https://scholarsmine.mst.edu/masters_theses/5252

This thesis is brought to you by Scholars' Mine, a service of the Missouri S&T Library and Learning Resources. This work is protected by U. S. Copyright Law. Unauthorized use including reproduction for redistribution requires the permission of the copyright holder. For more information, please contact scholarsmine@mst.edu.

T 2115
C/1
68P

INFRARED RELATED SOLID STATE STUDIES

BY

DONALD GEORGE RATHBUN, 1935

A

132947

THESIS

submitted to the faculty of

THE UNIVERSITY OF MISSOURI AT ROLLA

in partial fulfillment of the requirements for the

Degree of

MASTER OF SCIENCE IN PHYSICS

Rolla, Missouri

1968

Approved by

Robert J. Bell

(advisor)

Wayne E. Jefft

K. G. Jayhan

ABSTRACT

Infrared reflectivity measurements have been made on single crystal CdS. Classical dispersion analysis has been used in an analysis of the data to obtain the index of refraction, the extinction index, and the dispersion parameters. These are compared with previously published results. The procedure used in this analysis has been outlined for future reference.

Also, the shallow donor impurity theory has been used to numerically calculate the d_{+1} levels for Si and Ge. The theory is extended for the case of the impurity in the bulk semiconductor and the d_0 , d_{+2} and, for high n , the s , p_0 , and p_{+1} levels are found. Generalized energy equations, trial wave functions, effective Bohr radii, and some relative electric-dipole transition probabilities are given.

In addition, the longitudinal optical phonon-plasmon interaction theory of Varga is compared with experiment for several concentrations of Ga doped CdS. Phonon damping is introduced in the Varga dielectric function resulting in a more realistic reflectivity over the entire resonance region.

Finally, transmittance measurements have been made on "Cer-vit" glass-ceramic between 0.1920 and 1200 micrometers. The index of refraction is calculated from the observed channel spectra in the region between 200 and 1200 micrometers.

ACKNOWLEDGEMENT

The author wishes to thank his major professor, Dr. R.J. Bell, for his invaluable assistance in conducting the research included in this thesis. He also wishes to thank the staff of the Materials Research Center for the use of their equipment in conducting a portion of this research. Acknowledgement is also extended to T. McMahon and Dr. R.M. Fuller for helpful discussions, to Owens-Illinois Company for samples of "Cer-vit" glass-ceramic, and to all the others, too numerous to mention, who helped in the successful completion of this thesis.

TABLE OF CONTENTS

	Page
LIST OF FIGURES	v
LIST OF TABLES	vi
SECTION A: FAR INFRARED OPTICAL CONSTANTS IN CADMIUM SULFIDE.....	1
I. INTRODUCTION	2
II. THEORY	4
III. EXPERIMENT AND RESULTS	11
REFERENCES	18
SECTION B: SURFACE AND BULK IMPURITY EIGENVALUES IN THE SHALLOW DONOR IMPURITY THEORY.....	20
I. INTRODUCTION	21
II. TRIAL WAVE FUNCTIONS, ENERGY EQUATIONS, AND TRANSITION PROBABILITIES	23
III. CALCULATION OF THE $3d_{+1}$ EIGENVALUE	26
IV. CONCLUSION	37
V. ACKNOWLEDGEMENTS	39
ADDENDUM	40
REFERENCES	41
SECTION C: LONGITUDINAL OPTICAL PHONON-PLASMON COUPLING IN CdS.....	42
I. INTRODUCTION	43
II. REFLECTIVITY VS WAVELENGTH	44
III. REFLECTIVITY MINIMA	51
IV. DISCUSSION	53
REFERENCES	54
SECTION D: TRANSMITTANCE OF CER-VIT GLASS-CERAMIC IN THE ULTRAVIOLET, VISIBLE, INFRARED, AND SUBMILLIMETER WAVELENGTH REGIONS.....	55
REFERENCES	61
VITA	62

LIST OF FIGURES

Figures	Page
Section A	
1. Computer program for classical dispersion analysis	15
2. Reflectance vs wavenumber	16
3. Index of refraction and extinction index vs wavenumber	17
Section C	
1. Percent reflectivity vs wavelength for undoped CdS	48
2. Percent reflectivity vs wavelength for Ga-doped CdS. $N=1.0 \times 10^{18} \text{ cm}^{-3}$	49
3. Percent reflectivity vs wavelength for Ga-doped CdS. $N=1.5 \times 10^{19} \text{ cm}^{-3}$	50
4. Wavelength at reflectivity minimum vs impurity concentration for Ga-doped CdS	52
Section D	
1. Transmittance of Cer-Vit glass-ceramic in the ultraviolet, visible, and infrared wavelength regions	59
2. Transmittance of Cer-Vit glass-ceramic in the submillimeter wavelength region	60

LIST OF TABLES

Table		Page
	Section B	
1.	Sample trial wave functions	25
2.	Variational energy equations	29
3.	Effective Bohr radii	31
4.	Silicon eigenvalues	32
5.	Germanium eigenvalues	34
6.	Calculated optical relative radiative transition probabilities (silicon)	35
	Section D	
1.	Index of refraction	58

SECTION A

FAR INFRARED OPTICAL CONSTANTS
IN CADMIUM SULFIDE

I. INTRODUCTION

Classical dispersion analysis is commonly used as a method for determining the optical properties of non-conducting materials in the region of their absorption bands and has been defined⁽¹⁾, in general, as "the full specification of the oscillators required to give agreement with reasonably accurate optical data extending over some wavelength range." The main results of such an analysis are a determination of the optical constants of the material. These are the index of refraction, n , and the extinction index, K , which are, respectively, the real and imaginary parts of the complex index of refraction $n_c = n + iK$. The extinction index, K , is a measure of the absorption of incident radiation with the depth of penetration, x , in the material. It is related to the absorption coefficient, α , by the relation $\alpha = 4\pi K/\lambda$ which appears in the exponential law of absorption⁽²⁾ $I_x = I_0 e^{-\alpha x}$ and λ is the wavelength in vacuum. The theory to be developed will show that in the region of absorption resonances, n and K are not constants, as their title implies, but are rapidly varying functions of wavelength. The purpose of this study is the determination of these optical constants for cadmium sulfide in the region of its main infrared absorption band, 200 cm^{-1} -- 480 cm^{-1} .

Because of the complex nature of this type of analysis, it is not very practical without the use of high speed computers. Consequently, little work was done in this area until a few years ago when the necessary computers became available. However, the validity of this form of analysis was demonstrated quite some time ago by the work of Czerny⁽¹⁾ on NaCl. More recently,

dispersion analysis has been applied to SiC⁽³⁾, ZnO⁽⁴⁾, GaP⁽⁵⁾, MgF₂ and ZnF₂⁽⁶⁾, BN and BP⁽⁷⁾, quartz⁽¹⁾, and CdS and ZnS⁽⁸⁾. Verleur and Barker^{(9), (10)} have performed a similar type analysis on GaAs_yP_{1-y} and CdSe_yS_{1-y} alloys using a harmonic oscillator model developed to account for the significant features of the spectra of those particular alloys.

The dispersion analysis, by itself, yields the values of four dispersion parameters which are then used to obtain the optical constants. These parameters; the resonance frequency (ω_T), the resonance strength (ρ), resonance width (Γ), and low frequency dielectric constant (ϵ_0) are determined by a curve fitting procedure which involves the trial and error adjustment of the four parameters until the dispersion theory best fits the reflectivity data. The curve fitting procedure will be explained and the resulting optical constants and dispersion parameters compared with those obtained by Balkanski⁽⁸⁾ and Collins⁽¹¹⁾.

II. THEORY

Classical dispersion theory evolves from a consideration of the motion of a single elastically bound electron of an atom in a lattice and which has a resonant frequency ω_T . It applies equally well to the modes of vibration in an ionic crystal which has some degree of ionicity, such as CdS. The remainder of the theoretical development will be presented in this context. The motion to be considered is caused by some incident electromagnetic radiation which is assumed to be monochromatic and plane with frequency ω . The electric field at the ion sites can be expressed in complex notation as

$$\vec{E} = \vec{E}_0 e^{-i\omega t} \quad (1)$$

so that the driving force causing the motion of the ions is represented by

$$\vec{F} = -e \vec{E}_0 e^{-i\omega t} \quad (2)$$

Even though the electric and magnetic fields of the incident radiation are equal in magnitude, the force due to the magnetic field $(-e \dot{\vec{S}} \times \vec{B})/C$ is neglected because the ion velocity is very small in comparison to the velocity of light. The value \vec{S} will be considered as the displacement distance of an ion from its equilibrium position.

The other forces considered as acting on the ions are an elastic force of Hooke's law type, $-m\omega_T^2 \vec{S}$, and a viscous drag force, $-m\Gamma \frac{d\vec{S}}{dt}$ due to the effect of neighboring ionic charges on the motion of the ion. Combining these forces results in a differential equation of motion

$$\frac{d^2 \vec{S}}{dt^2} = -\Gamma \frac{d\vec{S}}{dt} - \omega_T^2 \vec{S} - \frac{e}{m} \vec{E}_0 e^{-i\omega t} \quad (3)$$

which has been divided through by m , the reduced mass of the ions.

Assuming a solution of the form

$$\vec{S} = \vec{S}_0 e^{-i\omega t} \quad (4)$$

so that

$$\frac{d\vec{S}}{dt} = -i\omega\vec{S}_0 e^{-i\omega t} = -i\omega\vec{S}$$

$$\frac{d^2\vec{S}}{dt^2} = -\omega^2\vec{S}_0 e^{-i\omega t} = -\omega^2\vec{S}$$

and substituting into the equation of motion gives

$$-\omega^2\vec{S}_0 + \omega_T^2\vec{S}_0 - i\omega\Gamma\vec{S}_0 = -\frac{e}{m}\vec{E}_0$$

$$(\omega_T^2 - \omega^2 - i\omega\Gamma)\vec{S}_0 = -\frac{e}{m}\vec{E}_0$$

$$\vec{S}_0 = \frac{-(e/m)\vec{E}_0}{(\omega_T^2 - \omega^2 - i\omega\Gamma)} \quad (5)$$

The solution of Maxwell's equations for monochromatic plane waves existing in a homogeneous medium⁽¹²⁾ yields an equation

$$n_c^2 = \epsilon\mu + i\frac{4\pi\mu\sigma}{\omega} \quad (6)$$

where μ is the magnetic permeability, ϵ is the dielectric constant, σ is the conductivity, and n_c is the complex index of refraction defined by

$$n_c = n + iK \quad (7)$$

with n the refractive index and K the extinction index.

For all non-magnetic media at very high frequencies, the electric field has a much greater effect than the magnetic field so the magnetic permeability will be taken as unity. By considering a non-conducting medium, the conductivity can be considered as zero, so that the second term in equation (6) is eliminated. This results in

$$n_c^2 = \epsilon \quad (8)$$

with ϵ complex.

An expression for ϵ is given⁽¹²⁾ as

$$\epsilon = 1 + 4\pi N\alpha \quad (9)$$

where N is the number of ionic dipoles per unit volume and α is the polarizability. The value of the high frequency dielectric constant, ϵ_∞ is taken as one here since $\epsilon \rightarrow 1$ as $\omega \rightarrow \infty$. However, at ultraviolet and visible light frequencies, the core electrons respond to incident photons and make a contribution.

It is customary to add this core electron contribution and label the resultant

ϵ_∞ giving

$$\epsilon = \epsilon_\infty + 4\pi N\alpha \quad (10)$$

It should be pointed out here that several^{(1), (3), (5)} of the papers in the field speak of the dielectric constant in terms of wavelength and, therefore, use ϵ_∞ as the low frequency or static dielectric constant and ϵ_0 as the high frequency dielectric constant.

Now, the dipole moment \vec{P} is given by⁽¹⁴⁾

$$\vec{P} = \alpha \vec{E} \quad (11)$$

and the dipole moment of the ionic pair⁽¹³⁾ is

$$\vec{P} = -e\vec{S} \quad (12)$$

Comparison of equations (11) and (12) results in

$$\alpha = \frac{-e|\vec{S}|}{|\vec{E}|} \quad (13)$$

Substituting the value of \vec{S} , found as a solution of the equation of motion, into equation (13) gives

$$\alpha = \frac{-e^2/m}{\omega^2 - \omega_T^2 + i\Gamma\omega} \quad (14)$$

Combining equations (8), (10), and (14) yields

$$n_c^2 = \epsilon_\infty - \frac{(4\pi Ne^2)/m}{\omega^2 - \omega_T^2 + i\Gamma\omega} \quad (15)$$

or, using equation (7)

$$n^2 - K^2 + i2nK = \epsilon_\infty - \frac{(4\pi Ne^2)/m}{\omega^2 - \omega_T^2 + i\Gamma\omega} \quad (16)$$

Separating the expression on the right into its real and imaginary parts results

in

$$n^2 - K^2 + i2nK = \epsilon_\infty - \frac{(4\pi Ne^2/m)(\omega^2 - \omega_T^2)}{(\omega^2 - \omega_T^2)^2 + \Gamma^2\omega^2} + \frac{i(4\pi Ne^2\Gamma\omega/m)}{(\omega^2 - \omega_T^2)^2 + \Gamma^2\omega^2} \quad (17)$$

Equating real and imaginary parts and rearranging results in

$$n^2 - K^2 = \epsilon_{\infty} + \frac{(4\pi Ne^2/m\omega_T^2) [1 - (\omega/\omega_T)^2]}{[1 - (\omega/\omega_T)^2]^2 + (\Gamma/\omega_T)^2 (\omega/\omega_T)^2} \quad (18)$$

$$2nK = \frac{(4\pi Ne^2/m\omega_T^2) (\omega/\omega_T) (\Gamma/\omega_T)}{[1 - (\omega/\omega_T)^2]^2 + (\Gamma/\omega_T)^2 (\omega/\omega_T)^2} \quad (19)$$

The oscillator strength, ρ , is given by

$$\rho = \frac{Ne^2}{m\omega_T^2} \quad (20)$$

This ρ differs from the expression given by Spitzer, Kleinman, and Walsh⁽³⁾ by a factor of $1/4\pi^2$ because they used a coefficient of $2\pi m\Gamma$ instead of $m\Gamma$ in the viscous drag term in the equation of motion. According to them

$$\epsilon_0 = \epsilon_{\infty} + 4\pi X \quad (21)$$

and

$$X = \rho \frac{1 - \omega^2}{(1 - \omega^2)^2 + \Gamma^2 \omega^2} \quad (22)$$

where X is the susceptibility. In the limit as ω goes to zero, X goes to ρ so that

$$\epsilon_0 = \epsilon_{\infty} + 4\pi\rho \quad (23)$$

Equations (18) and (19) can now be written

$$n^2 - K^2 = \epsilon_{\infty} + \frac{(\epsilon_0 - \epsilon_{\infty}) [1 - (\omega/\omega_T)^2]}{[1 - (\omega/\omega_T)^2]^2 + (\Gamma/\omega_T)^2 (\omega/\omega_T)^2} \quad (24)$$

$$2nK = \frac{(\epsilon_0 - \epsilon_\infty) (\omega/\omega_T) (\Gamma/\omega_T)}{[1 - (\omega/\omega_T)^2]^2 + (\Gamma/\omega_T)^2 (\omega/\omega_T)^2} \quad (25)$$

Now let

$$A = \epsilon_\infty + \frac{(\epsilon_0 - \epsilon_\infty) [1 - (\omega/\omega_T)^2]}{[1 - (\omega/\omega_T)^2]^2 + (\Gamma/\omega_T)^2 (\omega/\omega_T)^2} \quad (26)$$

$$B = \frac{1/2 (\epsilon_0 - \epsilon_\infty) (\omega/\omega_T) (\Gamma/\omega_T)}{[1 - (\omega/\omega_T)^2]^2 + (\Gamma/\omega_T)^2 (\omega/\omega_T)^2} \quad (27)$$

and solve for n and K in terms of A and B

$$n^2 - K^2 = A$$

$$nK = B$$

then $n = B/K$

$$(B/K)^2 - K^2 = A$$

$$K^4 + AK^2 - B^2 = 0$$

$$K^2 = \frac{-A + (A^2 + 4B^2)^{1/2}}{2} \quad (28)$$

$$n^2 = A + K^2 \quad (29)$$

The sign of the radical is taken as positive so that K will be positive.

Values of A and B can be obtained for a range of frequencies by guessing values of ϵ_0 , ω_0 , and Γ with ϵ_∞ being taken from available literature. From these values of A and B , the optical constants, n and K , can be calculated.

The reflectivity at ⁽¹⁴⁾ normal incidence

$$R = \frac{(n - K)^2 + K^2}{(n + K)^2 + K^2} \quad (30)$$

over the range of frequencies can now be calculated and compared to experimental values of reflectivity in the same range. The dispersion parameters are successively adjusted until the best fit of the calculated reflectivity to experimental reflectivity is obtained.

III. EXPERIMENT AND RESULTS

A single crystal of high purity cadmium sulfide was polished by standard optical polishing procedures with the c-axis perpendicular to the polished surface.

Reflectivity measurements were made at room temperature at near normal incidence from 200 cm^{-1} to 480 cm^{-1} with a Beckman IR-12 spectrophotometer. The sample compartment was purged with dry air to eliminate the atmospheric water vapor absorption bands. The reflectivity of a highly polished sample of bulk aluminum was measured for use as a reference since aluminum has a reflectivity of 96%⁽²⁾ in this region. Both of these measurements were made with unpolarized radiation.

A computer program was developed to perform the trial and error variation of the dispersion parameters necessary to fit the dispersion theory to the cadmium sulfide reflectivity data, which was adjusted to the aluminum reflectivity as a reference. This program is given in Fig. 1.

The treatment of dispersion analysis given is only for plane electromagnetic waves which are transverse so the resonant frequency, ω_T , of the ion refers to the transverse optical phonon resonance. This is pointed out by Kittel⁽¹⁵⁾, who also shows, by an analysis of the real part of the dielectric constant, the existence of a forbidden frequency region

$$\omega_T^2 < \omega^2 < \omega_L^2$$

where ω_L is the upper bound of the forbidden band of frequencies and is the

longitudinal optical phonon frequency. This treatment leads to the Lyddane-Sachs-Teller relation⁽¹⁶⁾

$$\frac{\epsilon(0)}{\epsilon(\infty)} = \frac{\omega_L^2}{\omega_T^2} \quad (31)$$

which is useful in determining a starting value of ϵ_0 for the dispersion analysis.

The value ω_T can be estimated quite closely as the steepest point on the long wavelength side of the reflectivity curve. The value of ω_L can be estimated as the value of ω where the experimental reflectivity goes to zero. The value of ϵ_∞ can be obtained from the literature or from reflectivity data in a high frequency region where there is no absorption for which K goes to zero so

$$\text{that } \epsilon_\infty = n^2 \quad (32)$$

$$\text{and } R = \frac{(n-1)^2}{(n+1)^2} \quad (33)$$

Other criteria for the initial determination of the dispersion parameters are given by Spitzer, Kleinman, and Walsh.⁽³⁾

A value for ϵ_∞ of 5.2 was obtained⁽¹⁷⁾ from the work of Piper and Marple.⁽¹⁸⁾ Values of ϵ_0 and ω_T were estimated using the procedure outlined above. A value for Γ was picked at random and tried. Since the values of ϵ_∞ , ϵ_0 , and ω_T were considered to be fairly accurate, the value of Γ was varied by itself to determine its effect on the theoretical curve. It was found that the value of Γ had the effect of varying the height of the reflectivity peak as well as the halfwidth of the peak. As the value of Γ was decreased below

a certain range of values, it was found to have very little further effect on the peak maximum value but still caused changes in the halfwidth. A final value of $\Gamma = 4.0 \text{ cm}^{-1}$ was chosen to best fit the halfwidth of the experimental data. In all cases, the calculated reflectivity peak was less than the experimental peak.

The initial value of ω_T chosen was 242 cm^{-1} which was quite accurate and was used throughout the analysis. It agrees with the value of 241 cm^{-1} of Balkanski, et. al. ⁽⁸⁾, 241 cm^{-1} by Collins ⁽¹¹⁾ and 242 cm^{-1} by Tell, Damen, and Porto ⁽¹⁹⁾ using Raman techniques.

The initial value of ϵ_0 was found to be a little high and was finally adjusted to a value of 8.27. As might be expected from the theory, changing the value of ϵ_0 , changes the position of the reflectivity minimum with smaller values moving the minimum toward smaller wavenumber or longer wavelength. This value of $\epsilon_0 = 8.27$ is somewhat lower than the value of 8.6 of Balkanski and 9.3 of Collins.

It should be pointed out that the value of $\epsilon_\infty = 5.2$ was not varied and is lower than the values reported by Balkanski, Collins, and Verleur and Barker. ⁽¹⁰⁾ It is suggested, that if further work is done in this area, that the value of ϵ_∞ also be adjusted to determine its effect on the data fit.

As a further attempt to better fit the data, a computer program was written for a system using two harmonic oscillators instead of one. It was not considered as successful in this case because the fit obtained was not any

better than that using the single oscillator model. The best fit to the data using the double oscillator model was obtained with the resonant frequencies quite close together indicating the likelihood of only one oscillator.

The fit obtained between the reflectivity data and the theoretical curve is shown as Fig. 2 and the resulting curves of n and K are given as Fig. 3. The general shape of the curves closely approximate the results of Balkanski, et. al.⁽⁸⁾

It is seen that the data fit near the peak of the resonance is not very accurate. In fact, the shape of the two peaks are somewhat assymmetric. An effect of this nature has been explained by Kleinman and Spitzer⁽⁵⁾ as being due to the polishing of the reflectivity surface. They speculate that the polishing of the surface in some way damages the crystal surface so that the reflectivity observed is not the reflectivity characteristic of the bulk material. The effect of etching after polishing is seen to change the shape to more generally coincide with the shape of the theoretical peak.

As a final note, it should be stated that the values of n and K should be obtained from equations (28) and (29). If the value of n is obtained from the relation $n = B/K$, it is found to be very erratic because the values of K are, in general, so small that the computer program becomes quite inaccurate.

```

C      SINGLE RESONANCE  CADMIUM SULFIDE
      DOUBLE PRECISION  GAMMA, GNU, SI, ART, WAVE, DWAVE,
*     RATIO, ANT, BILL, CAT, DOG, FIGHT, A, B, CAYSQR, ENSQR,
*     CAY, EN, R, DSQRT, EINF, EDIFF, EZERO
      EINF=5.2
      EZERO=8.27
      EDIFF=(EZERO-EINF)
      GAMMA=4.
      GNU=242.
      SI=GAMMA/GNU
      ART=SI*SI
      WAVE=200.
      DWAVE=5.
      DO 1 I=1,101
      RATIO=WAVE/GNU
      ANT=RATIO*RATIO
      BILL=1. -ANT
      CAT=BILL*BILL
      DOG=ANT*ART
      FIGHT=CAT+DOG
      A=EINF+( ( BILL*EDIFF)/FIGHT)
      B=(EDIFF*RATIO*SI)/FIGHT
      ENSQR=(A+DSQRT(A*A+B*B))/2
      EN=DSQRT(ENSQR)
      CAYSQR=(DSQRT(A*A+4.*B*B))/2
      CAY=DSQRT(CAYSQR)
      R=(ENSQR-2.*EN+1. +CAYSQR/
* (ENSQR+2.*EN+1. +CAYSQR)
      WRITE (3,100)WAVE, R, EN, CAY
1     WAVE=WAVE+DWAVE
      STOP
100    FORMAT(F6.1, 3F10.6)
      END
/ DATA

```

Figure 1: Computer Program for Classical Dispersion Analysis

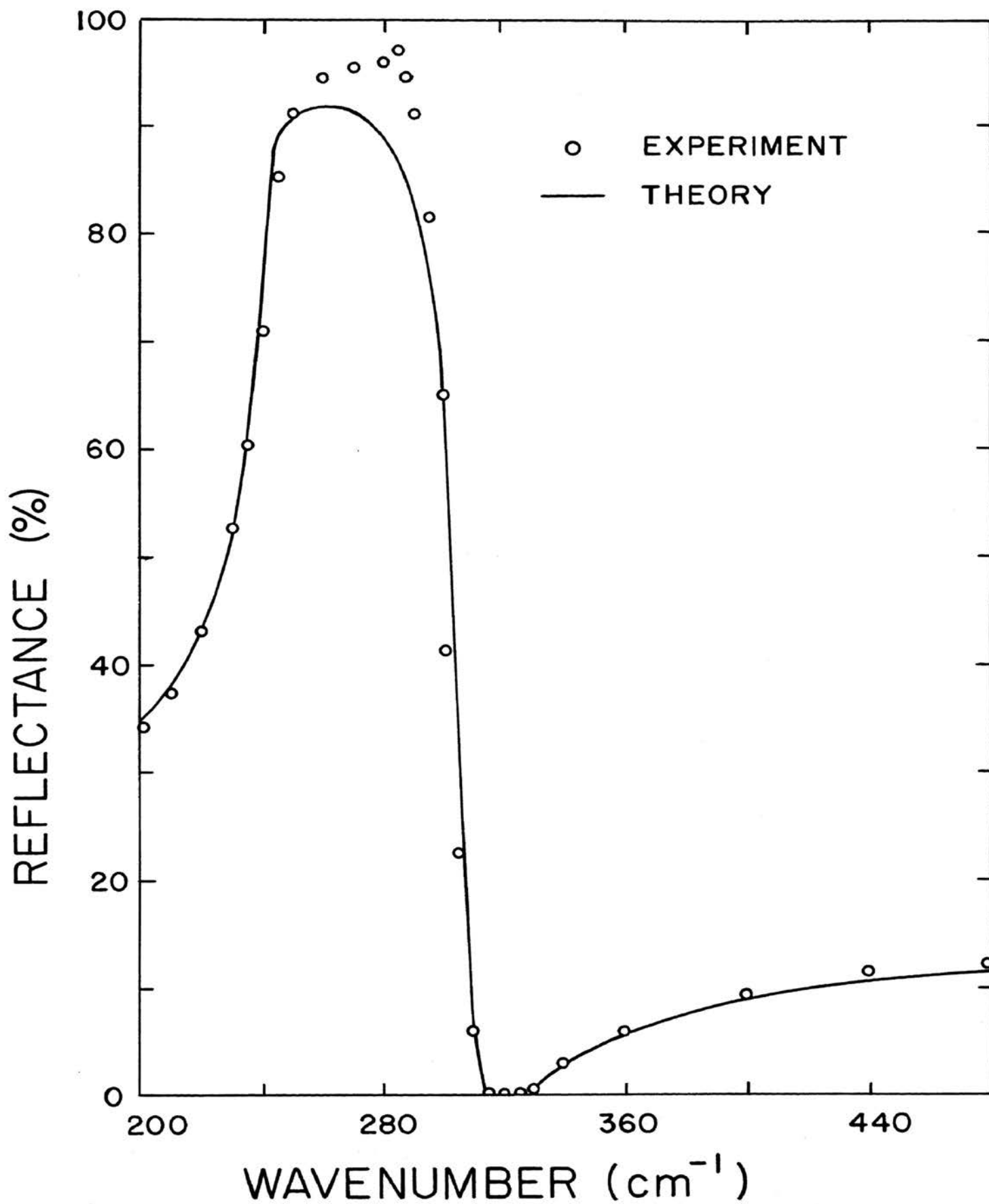


Figure 2: Reflectance vs wavenumber

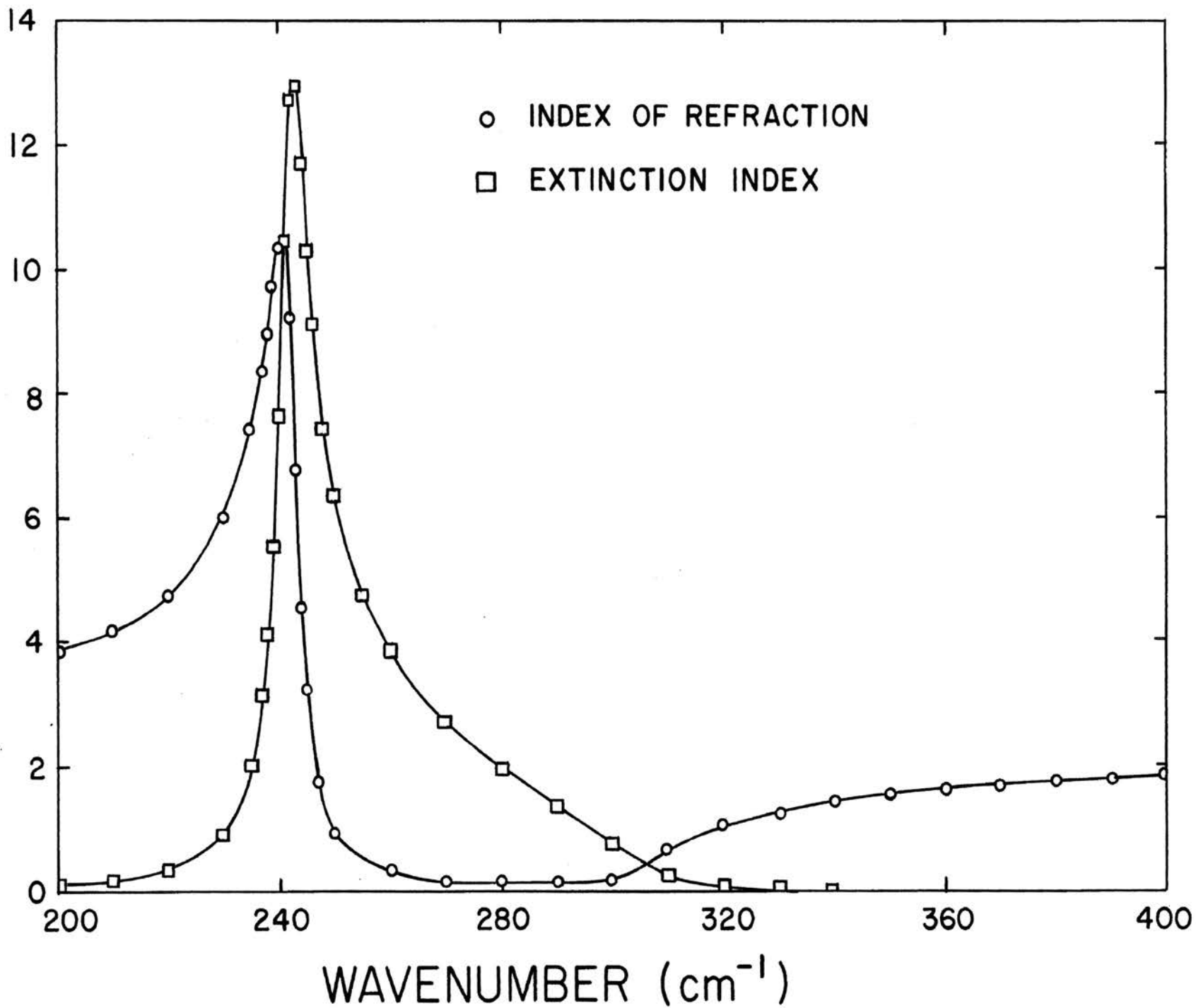


Figure 3: Index of refraction and extinction index vs wavenumber

REFERENCES

1. Spitzer, W.G. and Kleinman, D.A., "Infrared Lattice Bands of Quartz." Phys. Rev. 121, 1324-1335 (1961).
2. Jenkins, F.A. and White, H.E., Fundamentals of Optics, McGraw-Hill, New York (1957).
3. Spitzer, W.G., Kleinman, D. and Walsh, D., "Infrared Properties of Hexagonal Silicon Carbide" Phys. Rev. 113, 127-132 (1959).
4. Collins, R.J. and Kleinman, D., "Infrared Reflectivity of Zinc Oxide" J. Phys. Chem. Solids 11, 190-194 (1959).
5. Kleinman, D.A. and Spitzer, W.G., "Infrared Lattice Absorption of GaP" Phys. Rev. 118, 110-117 (1960).
6. Barker, Jr., A.S., "Transverse and Longitudinal Optic Mode Study in MgF_2 and ZnF_2 ." Phys. Rev. 136A, 1290-1295 (1964).
7. Gielisse, P.J., Mitra, S.S., Plendi, J.N., Griffis, R.D., Mansur, L.C., Marshall, R., and Pascoe, E.A., "Lattice Infrared Spectra of Boron Nitride and Boron Monophosphide." Phys. Rev. 155, 1039-1046 (1967).
8. Balkanski, M., Nusimovici, M., and LeToullec, R., "Interaction Du Champ De Rayonnement Avec Des Phonons Simples et Multiples Dans Les Structures Du Type Wurtzite et Blende," J. De Physique 25, 305-316 (1964).
9. Verleur, H.W. and Barker, Jr., A.S., "Infrared Lattice Vibrations in $GaAs_{1-y}P_y$ Alloys" Phys. Rev. 149, 715-729 (1966).
10. Verleur, H.W. and Barker, Jr., A.S., "Optical Phonons in Mixed Crystals of $CdSe_{1-y}S_y$ " Phys. Rev. 155, 750-763 (1967).
11. Collins, R.J., "Mechanism and Defect Responsible for Edge Emission in CdS." J. of Appl. Phys. 30, 1135-1140 (1959).
12. Stone, J.M., Radiation and Optics, McGraw-Hill, New York, Chap. 15 (1963).
13. Stone, J.M., Radiation and Optics, McGraw-Hill, New York, Chap. 14 (1963).
14. Stone, J.M., Radiation and Optics, McGraw-Hill, New York, Chap. 16 (1963).
15. Kittel, C., Introduction to Solid State Physics 3rd ed, Wiley, New York, Chap. 5 (1966).

16. Lyddane, R.H., Sachs, R.G., and Teller, E., "On the Polar Vibrations of Alkali Halides" Phys. Rev. 59, 673-676 (1941).
17. Bell, R.J., Private Communication.
18. Piper, W.W. and Marple, D.T.F., "Optical Properties of Free Electrons in CdS." J. Appl. Phys. Suppl. 32, 2237-2241 (1961).
19. Tell, B., Damen, T.C., and Porto, S.P.S., "Raman Effect in Cadmium Sulfide." Phys. Rev. 144, 771-774 (1966).

SECTION B

SURFACE AND BULK IMPURITY EIGENVALUES IN THE
SHALLOW DONOR IMPURITY THEORY*

Robert J. Bell, Physics Department and
Graduate Center for Materials Research
University of Missouri at Rolla
Rolla, Missouri

W. T. Bousman, Jr., Physics Department, University of Missouri at Rolla
Rolla, Missouri

G. M. Goldman, Physics Department, University of Missouri at Rolla
Rolla, Missouri

D. G. Rathbun, Physics Department, University of Missouri at Rolla
Rolla, Missouri

*Contribution number 10 from Graduate Center for Materials Research

I. INTRODUCTION

In a recent article by Levine⁽¹⁾ the shallow donor impurity problem was theoretically treated for the case for which the impurity is located at the semiconductor surface. In Levine's theory it is assumed that the work function is infinite compared to the impurity ionization energy, that the Bloch functions hold right to the surface and that the ion is exactly at the clean surface. The principal results for the surface problem obtained by Levine are that a state cannot exist unless $l + m$ is an odd integer and that both l and m must differ by ± 1 in an electromagnetic transition. l and m are respectively the "orbital" and "magnetic" quantum numbers in the hydrogenic-like approximations. For the case of the impurity nuclei at the semiconductor surface, one then finds that the ground state becomes the $2p_0$ level since no s levels can exist. Also the first states to which a transition might be observed in absorption are the $3d_{\pm 1}$ and $4d_{\pm 1}$ states.

As part of an experimental program of studying the energy level structure for shallow donor impurities when the nucleus is at the surface, the $d_{\pm 1}$ level values are calculated for silicon and germanium. The trial wave function is given, and some of the details of the variational calculation are presented.

Another shallow donor problem is to extend the calculation of the eigenvalues of p_0 and $p_{\pm 1}$ levels for the case when the impurity is in the bulk semiconductor. Recent infrared experiments⁽²⁾⁽³⁾⁽⁴⁾ have located the $4p_0$, $5p_0$, $4p_{\pm 1}$, and $5p_{\pm 1}$ levels and it is of interest to see the comparison between experiment and theory for these levels.

Also these recent experiments have shown some weak transitions which as yet have not been accounted for.^{(3), (4)} An attempt to correlate these lines with the first order forbidden $1s$ to d_0 , d_{+1} , and d_{+2} levels seemed worthwhile in light of the fact that $1s$ to $2s$ transitions have been observed⁽³⁾ though those transitions are also forbidden.

II. TRIAL WAVE FUNCTIONS, ENERGY EQUATIONS, AND TRANSITION PROBABILITIES

Much work in the mid 1950's was done by Kleiner,⁽⁵⁾ Lampert,⁽⁶⁾ Kohn and Luttinger,⁽⁷⁾ Kittel and Mitchell⁽⁸⁾ and by Kohn^{(9), (10)} on the choice of trial wave functions for the bulk shallow donor impurity problem. The work culminated when Lampert,⁽⁶⁾ Kleiner⁽⁵⁾ and Kohn⁽¹⁰⁾ gave for the 1s state the trial function

$$\Psi = (A^2 B / \pi)^{1/2} \exp (- [A^2 (x^2 + y^2) + B^2 z^2]^{1/2}) \quad (1)$$

for the anisotropic effective mass problem. This was given as a trial function to be compared with an isotropic effective mass wave function⁽¹¹⁾ of

$$\Psi = (1/\pi a_o^3)^{1/2} \exp (-r/a_o) \quad (2)$$

In these equations $1/A$ and $1/B$ are two constants - "effective" Bohr radii - to be determined from variational calculations⁽¹⁰⁾ and a_o is the Bohr radius. However, the details of the variational calculation itself were left out of press. For the excited state problems Brown, Kleiner, and Lax⁽¹²⁾ reported at Cambridge, Massachusetts meeting some information and Lax⁽¹³⁾ later gave in print an indication of the form of the trial functions. Since these normalized wave functions are not completely and explicitly set down anywhere with the normalizing constants it seems worthwhile to give some examples in Table I. In obtaining the trial functions the following substitutions in the isotropic mass hydrogen atom wave functions were made:

$$a_o^3 \longrightarrow 1/A^2 B \quad (3)$$

in the normalization and in the functional variation:

$$r/a_0 = \left[A^2(x^2 + y^2) + B^2z^2 \right]^{1/2} \quad (4)$$

$$(r/a_0) \sin \theta \cos \phi = xA \quad (5)$$

$$(r/a_0) \sin \theta \sin \phi = yA \quad (6)$$

$$(r/a_0) \cos \theta = zB. \quad (7)$$

One point which is important is that these trial functions are normalized.

Table 1

Sample Trial Wave Functions	
State	Trial Wave Function, $[\dots] = [\rho^2 A^2 + z^2 B^2]$
1s	$\left(\frac{A^2 B}{\pi}\right)^{1/2} \exp\{-[\dots]^{1/2}\}$ (a)
2p ₀	$\left(\frac{A^2 B}{32\pi}\right)^{1/2} zB \exp\{-\frac{1}{2}[\dots]^{1/2}\}$
2p _{<u>±</u>1}	$\left(\frac{A^2 B}{64\pi}\right)^{1/2} (x \pm iy) A \exp\{-\frac{1}{2}[\dots]^{1/2}\}$
3d ₀	$\left(\frac{A^2 B}{6\pi(8l)}\right)^{1/2} 2\{3B^2 z^2 - [\dots]\} \exp\{-\frac{1}{3}[\dots]^{1/2}\}$
3d _{<u>±</u>1}	$\left(\frac{A^2 B}{(8l)^2 \pi}\right)^{1/2} (x \pm iy) AzB \exp\{-\frac{1}{3}[\dots]^{1/2}\}$
3d _{<u>±</u>2}	$\left(\frac{A^2 B}{(162)^2 \pi}\right)^{1/2} \{(x^2 - y^2) A^2 \pm i(2xy) A^2\} \exp\{-\frac{1}{3}[\dots]^{1/2}\}$

(a) See reference (6)

III. CALCULATION OF THE $3d_{+1}$ EIGENVALUE

From Table 1 it is seen that the trial function for the $3d_{+1}$ level can be written as

$$\Psi = (A^2 B / (8l)^2 \pi)^{1/2} (zB) (x + iy)A \exp \left\{ - \left[\frac{\dots}{3} \right]^{1/2} \right\} \quad (8)$$

The normalization for all A and B was proved by making the substitutions

$$\rho' = \rho A = ((x^2 + y^2) A^2)^{1/2} = R \sin \theta \quad (9)$$

and

$$Z' = zB = R \cos \theta \quad (10)$$

(after having noted the cylindrical symmetry in $\Psi^* \Psi$), letting

$$d\rho' \, d z' = R dr \, d\theta, \quad (11)$$

and noting that the limits on θ are zero and π (not 2π). Effectively, one needs integrate only in the upper half plane.

To obtain the eigenvalues, the trial wave function in rectangular coordinates was operated on by the Hamiltonian⁽¹⁰⁾

$$H = - \frac{\hbar^2}{2m_t} \left(\frac{\partial^2}{\partial x^2} + \frac{\partial^2}{\partial y^2} \right) - \frac{\hbar^2}{2m_l} \left(\frac{\partial^2}{\partial z^2} \right) - e^2 / K(x^2 + y^2 + z^2)^{1/2} \quad (12)$$

and inserted in

$$\langle E \rangle = \iiint \Psi^* H \Psi \, dx dy dz \quad (13)$$

to obtain the eigenvalue via the variational calculations. In the above equations m_l and m_t are the longitudinal and transverse effective masses found by cyclotron^{(10), (14), (15)} resonance and Zeeman⁽¹⁶⁾ experiments, e is the electronic charge, and K is the dielectric constant of the semiconductor.⁽¹⁰⁾ It was noted that cylindrical symmetry exists, and so the integral was converted to cylindrical

coordinates. Then the substitutions of equations (9), (10), and (11) separates the integrals into the product of one integral in θ and another in R in all cases.

All of the integrals encountered were simple and readily yielded:

$$\langle E \rangle = \frac{1}{9} \left\{ \frac{2\hbar^2 A^2}{7m_t} + \frac{3\hbar^2 B^2}{14m_l} - \frac{15 e^2 AB}{4K (B^2 - A^2)^{1/2}} \right. \\ \left. \times \left[\left(\frac{3a^2}{4} - \frac{1}{2} \right) (a^2 - 1)^{1/2} + \left(a^2 - \frac{3a^4}{4} \right) \sin^{-1} \left(\frac{1}{a} \right) \right] \right\} \quad (14)$$

where:

$$a^2 = B^2 / (B^2 - A^2) \quad (15)$$

It should be noted that the level is degenerate as it should be in $m = \pm 1$.

All the other energy equations were found in a similar fashion and the results are tabulated in Table 2. It is worth noting that the results obtained by explicitly calculating the $1s$, $2s$, $3s$, $2p_0$, $4p_0$, $5p_0$, $2p_{\pm 1}$, $4p_{\pm 1}$, $5p_{\pm 1}$, $3d$, $3d_{\pm 1}$, $4d_{\pm 1}$, and $3d_{\pm 2}$ levels can be expressed in a series of $1/n^2$.

The minimum value of $\langle E \rangle$ was then taken as the eigenvalues for both germanium and silicon. The minimum $\langle E \rangle$ value was obtained at different A and B values for the different type levels. Table 3 summarizes the results for all levels calculated for the solution of these problems.

Tables 4 and 5 summarize the numerical results found for silicon and germanium respectively. The results show that the energy levels have been correctly identified in the experimental papers, ^{(2), (3), (4)} that the d levels are not involved in the unidentified weak transitions, ^{(3), (4)} that the $2s$ level is calculated for germanium for the first time, and that Kleiner⁽⁵⁾ was accurate in his early calculations.

In addition, some relative electric-dipole transition probability calculations⁽¹⁷⁾ were made and the results are tabulated in Table 6. It is found for the $5p_0$ level that the transition would be very difficult to observe.

Table 2

Variational Energy Equations	
Type State	Energy Equation
s	$\frac{1}{n^2} \left\{ \frac{\hbar^2 A^2}{3m_t} + \frac{1}{6} \frac{\hbar^2 B^2}{m_l} - \frac{e^2}{K} \left[\frac{AB}{(B^2 - A^2)^{1/2}} \sin^{-1} \left(\frac{(B^2 - A^2)^{1/2}}{B} \right) \right] \right\}$
p ₀	$\frac{1}{n^2} \left\{ \frac{\hbar^2 A^2}{5m_t} + \frac{3\hbar^2 B^2}{10m_l} - \frac{3e^2 AB}{2K(B^2 - A^2)^{1/2}} \left[-\frac{A}{(B^2 - A^2)^{1/2}} + \frac{B^2}{B^2 - A^2} \right. \right.$ $\left. \left. \times \sin^{-1} \left(\frac{(B^2 - A^2)^{1/2}}{B} \right) \right] \right\}$
p ₊₁	$\frac{1}{n^2} \left\{ \frac{2\hbar^2 A^2}{5m_t} + \frac{\hbar^2 B^2}{10m_l} - \frac{3e^2}{4K} \frac{AB}{(B^2 - A^2)^{1/2}} \left[\frac{A}{(B^2 - A^2)^{1/2}} \right. \right.$ $\left. \left. + \left[\sin^{-1} \left(\frac{(B^2 - A^2)^{1/2}}{B} \right) \right] \frac{B^2 - 2A^2}{B^2 - A^2} \right] \right\}$
d ₀	$\frac{1}{n^2} \left\{ \frac{5\hbar^2 A^2}{21m_t} + \frac{11\hbar^2 B^2}{42m_l} - \frac{5e^2}{8K} \frac{AB}{(B^2 - A^2)^{1/2}} \left[\left(\frac{27}{4} a^4 - 6a^2 + 2 \right) \right. \right.$ $\left. \left. \times \sin^{-1} \left(\frac{1}{a} \right) - \left(\frac{27}{4} a^2 - \frac{3}{2} \right) (a^2 - 1)^{1/2} \right] \right\}$

Table 2 continued

$$d_{+1} = \frac{1}{n^2} \left\{ \frac{2\hbar^2 A^2}{7m_t} + \frac{3\hbar^2 B^2}{14m_l} - \frac{15e^2}{4K} \frac{AB}{(B^2 - A^2)^{1/2}} \left[(a^2 - \frac{3}{4}a^4) \right. \right.$$

$$\left. \left. \times \sin^{-1} \left(\frac{1}{a} \right) + \left(\frac{3}{4}a^2 - \frac{1}{2} \right) (a^2 - 1)^{1/2} \right] \right\}$$

$$d_{+2} = \frac{1}{n^2} \left\{ \frac{3\hbar^2 A^2}{7m_t} + \frac{\hbar^2 B^2}{14m_l} - \frac{15e^2}{16K} \frac{AB}{(B^2 - A^2)^{1/2}} \left[\left(\frac{3}{4}a^4 - 2a^2 + 2 \right) \right. \right.$$

$$\left. \left. \times \sin^{-1} \left(\frac{1}{a} \right) - \left(\frac{3}{4}a^2 - \frac{3}{2} \right) (a^2 - 1)^{1/2} \right] \right\}$$

NOTE: $a = B/(B^2 - A^2)^{1/2}$

Table 3

Effective Bohr Radii		
Silicon		
Type State	$\frac{1}{A}(\text{\AA})$	$\frac{1}{B}(\text{\AA})$
s	24.8 (a)	13.9 (a)
p_0	18.6	11.0
p_{+1}	28.0	16.8
d_0	20.7	10.5
d_{+1}	22.3	13.7
d_{+2}	29.5	18.3
Germanium		
s	64.6 (a)	22.8 (a)
p_0	40.3	15.4
p_{+1}	79.8	32.3
d_0	45.6	14.3
d_{+1}	56.0	23.2
d_{+2}	86.8	37.0

(a) See reference (10)

Table 4

Silicon Eigenvalues					
State	Theoretical	Eigenvalue (meV)			
		P(c)	As(c)	Li(d)	LiO(d)
1s	-28.6 (b)	-45.3	-53.5	-32.5	-39.2
2s	- 7.15 (b)			- 7.3	
3s	- 3.18				
4s	- 1.79				
5s	- 1.14				
6s	- 0.79				
2p ₀	-10.7 (b)	-10.9	-10.8		-11.0
3p ₀	- 4.74 (b)	- 4.9	- 4.9	- 4.9	- 5.0
4p ₀	- 2.68				
5p ₀	- 1.71				
6p ₀	- 1.19				
2p ₊₁	- 5.81 (b)	- 5.8	- 5.8	- 5.8	- 5.9
3p ₊₁	- 2.58 (b)	- 2.6	- 2.6	- 2.6	- 2.6
4p ₊₁	- 1.45	- 1.6	- 1.5	- 1.6	- 1.6
5p ₊₁	- 0.93	- 0.9	- 0.9	- 0.9	
6p ₊₁	- 0.65			- 0.3	

Table 4 continued

$3d_o$	- 4.50
$4d_o$	- 2.53
$5d_o$	- 1.62
$6d_o$	- 1.12
$3d_{-1}$	- 3.56
$4d_{-1}$	- 2.00
$5d_{-1}$	- 1.28
$6d_{-1}$	- 0.89
$3d_{+2}$	- 2.38
$4d_{+2}$	- 1.34
$5d_{+2}$	- 0.86
$6d_{+2}$	- 0.60

(b) See reference (5)

(c) See reference (2)

(d) See reference (3)

Table 5

Germanium Eigenvalues			
State	Eigenvalue (meV)	State	Eigenvalue (meV)
1s	-9.02 (a)	3d ₀	-1.87
2s	-2.25	4d ₀	-1.05
3s	-1.00	5d ₀	-0.67
4s	-0.56	6d ₀	-0.47
5s	-0.36		
6s	-0.25	3d ₊₁	-1.16
		4d ₊₁	-0.65
2p ₀	-4.38 (a)	5d ₊₁	-0.42
3p ₀	-1.94 (a)	6d ₊₁	-0.29
4p ₀	-1.09		
5p ₀	-0.70	3d ₊₂	-0.62
6p ₀	-0.49	4d ₊₂	-0.35
		5d ₊₂	-0.22
2p ₊₁	-1.59 (a)	6d ₊₂	-0.16
3p ₊₁	-0.70 (a)		
4p ₊₁	-0.40		
5p ₊₁	-0.25		
6p ₊₁	-0.18		

(a) See reference (10)

Table 6

Calculated Optical Relative Radiative Transition Probabilities (Silicon)					
Transition	Theoretical Relative Intensity	P(b)	As(b)	Li(c)	LiO(c)
1s to 2p ₀	0.39 (a), (b)	0.43	0.34		0.35
1s to 3p ₀	0.062 (a), (b)	0.17	0.13	0.17	0.10
1s to 4p ₀	0.021 (b)				
1s to 5p ₀	0.010				
1s to 6p ₀	0.0056				
1s to np ₀	$\exp(14.15 n^{-1/2} - 10.97)$				
1s to 2p ₊₁	1.00 (a), (b)	1.0	1.0	1.0	1.0
1s to 3p ₊₁	0.16 (a), (b)	0.66	0.56	0.55	0.45
1s to 4p ₊₁	0.055				
1s to 5p ₊₁	0.026				
1s to 6p ₊₁	0.015				
1s to np ₊₁	$\exp(14.15 n^{-1/2} - 9.94)$				
2p ₀ to 3d ₊₁	4.79				
2p ₀ to 4d ₊₁	0.80				
2p ₀ to 5d ₊₁	0.23				
2p ₀ to 6d ₊₁	0.094				
2p ₀ to nd ₊₁	$\exp(23.29 n^{-1/2} - 11.88)$				

Table 6 continued

-
- (a) See reference (10)
 - (b) See reference (2)
 - (c) See reference (3)

IV. CONCLUSION

Normalized trial wave functions for the anisotropic effective mass shallow donor theory have been given. A method of calculating the eigenvalues in closed form is given, and d levels are calculated for the first time, and for high n the s , p_0 , and p_{+1} levels are located. The anisotropy dependent values are expressible in $1/n^2$ series for the first time.

With a $2p_0$ ground state⁽⁷⁾ in the Levine theory⁽¹⁾ and using the $3d_{+1}$ energy value from Tables 4 and 5 the first observable transition energy for the surface ion problem will be about 3.2meV or equivalently about 390 microns wavelength in germanium. In silicon the same transition will be at about 7.1meV or 180 microns wavelength with a large relative transition probability (see Table 6).

These $2p_0$ to d_{+1} transitions will be sought in submillimeter wavelength absorption experiments on heavily surface doped n-type silicon and germanium samples at liquid helium temperatures. Since the transition energies are now known in the Levine theory both wavelength discrimination and impurity depth control can be used in these experiments to check Levine's theory and any possible departures can be positively confirmed and used for higher order approximations.

Since Levine's theory has so many approximations in it, one has to proceed with caution. One alternative to the approach used by Levine is to include the s levels in a "central cell" type calculation for the ions at the surface. However, this is a very difficult calculation for the surface problem and

the possibility is probably best checked first by experiment. One would vary the type of group V impurity at the surface and observe the change in the ionization energy. The "central cell" effect would show a changing ionization energy with changing impurity and Levine's theory predicts the same ionization energy. Also the "central cell" might be expected to produce a larger ionization energy than that found in Levine's theory and predicted in these calculations.

For wave functions other than the $1s$, $2p_0$, $2p_{\pm}$, and $3d_{\pm}$ -like wave functions the approximations are so drastic that results involving them are of questionable significance. However, to do better may involve considerable effort, so that the results may, nevertheless, be of some value in comparing with experiment. The questionable approximations, in particular the fact that the energy eigenfunctions not listed above are not orthogonal to those listed, is thus pointed out.

V. ACKNOWLEDGMENTS

The authors wish to thank Drs. O. H. Hill, J. P. Wesley, J. L. Rivers, and H. A. Brown for helpful discussions. Also, several students of the Physics Department who checked some of the calculations are to be thanked.

- D. Scarpero and J. Boehmer -

ADDENDUM

In the anisotropic case the six 100 equivalent directions are normal to the semiconductor surface, the wave functions are multiplied by $2^{1/2}$ for half-space normalization, and the θ integral limit is $\pi/2$ for the surface problem.

References

- (1) J. D. Levine, Phys. Rev. 140, A586 (1965).
- (2) J. W. Bichard and J. C. Giles, Canadian J. Phys. 40, 1480 (1962).
- (3) T. E. Gilmer, Jr., R. K. Franks and R. J. Bell, J. Phys. Chem. Solids 26, 1195 (1965).
- (4) R. L. Aggarwal, P. Fisher, V. Mourzine, and A. K. Ramdas, Phys. Rev. 138, A882 (1965).
- (5) W. H. Kleiner, Phys. Rev. 97, 1722 (1955).
- (6) M. A. Lampert, Phys. Rev. 97, 352 (1952).
- (7) W. Kohn and J. M. Luttinger, Phys. Rev. 97, 1721 (1955).
- (8) C. Kittel and A. H. Mitchell, Phys. Rev. 96, 1488 (1954).
- (9) W. Kohn, Phys. Rev. 98, 1856 (1955).
- (10) W. Kohn, Solid State Physics 5, 257, Academic Press, Inc., N. Y. (1957).
- (11) L. Pauling and E. B. Wilson, Introduction to Quantum Mechanics, pp. 133, McGraw-Hill Book Co., N. Y. (1935).
- (12) W. H. Kleiner, R. N. Brown, and B. Lax, Bull. Amer. Phys. Soc. Ser. II, 4, 144 (1959).
- (13) Proceedings International School of Physics, Course XXII, Semiconductors, B. Lax, pp. 240, Academic Press, N. Y. (1963).
- (14) R. N. Dexter, B. Lax, A. F. Kip, and G. Dresselhaus, Phys. Rev. 96, 1222 (1954).
- (15) R. C. Fletcher, W. A. Yager, and F. R. Merritt, Phys. Rev. 100, 747 (1955).
- (16) S. Zwerdling, K. J. Button, and B. Lax, Phys. Rev. 118, 975 (1960).
- (17) L. I. Schiff, Quantum Mechanics, McGraw-Hill Book Company, N. Y. (1955).

SECTION C

Longitudinal Optical Phonon - Plasmon Coupling in CdS*

by

Robert J. Bell
Physics Department and
Graduate Center for Materials Research
University of Missouri at Rolla

Thomas J. McMahon[#]
Donald G. Rathbun
Physics Department
University of Missouri at Rolla

*Contribution number 28 from the Materials Research Center.

[#]U.S. Bureau of Mines Fellow.

I. INTRODUCTION

It is the purpose of this article to show that (1) the reflectivity versus wavelength data in the infrared of Piper and Marple⁽¹⁾ for doped CdS can be fairly well approximated by the theory for longitudinal optical phonon - plasmon interaction by Varga;⁽²⁾ (2) there is need for further infrared experimental work to examine a second reflectivity minimum predicted by Varga;⁽²⁾ and (3) the reflectivity minimum associated with the reststrahl peak can be reasonably accounted for over the entire range of impurity concentrations.

These experiments of Piper and Marple⁽¹⁾ were on the free carrier absorption in semiconductors; however, they published their actual data of the reflectivity versus wavelength. The concentration level and range of Ga doping in their CdS samples allows one to use their data to extract information concerning plasma interactions in solids.

With concentrations of free carriers in CdS in the range of 10^{18} cm^{-3} or greater, one might expect plasma effects in the solid. In particular, plasmon - phonon interactions are present as will be shown in the next section. This interaction will be with the longitudinal optical phonons since in the electrostatic approximation used by Born and Huang⁽³⁾ the electric field is equal to zero everywhere for transverse optical phonons but not for longitudinal optical phonons.

II. REFLECTIVITY VERSUS WAVELENGTH

In Figure 1-3 the data represented by circles are the reflectivity data of Piper and Marple⁽¹⁾ for Ga doped CdS. In Figure 1, in addition to the data of Piper and Marple, the undoped data of Collins⁽⁴⁾ is plotted as x's and Balkanski, et al.⁽⁵⁾ is plotted as □'s. These data are all from near normal incidence.

The solid lines are from the theoretical work of Varga. Varga's predictions are obtained from the reflectivity, R, given by

$$R = \left[\frac{(\epsilon_T(0, \omega))^{1/2} - 1}{(\epsilon_T(0, \omega))^{1/2} + 1} \right]^2 \quad (1)$$

where

$$\epsilon_T(0, \omega) = \epsilon_\infty + \frac{\epsilon_0 - \epsilon_\infty}{1 - \left(\frac{\omega}{\omega_t}\right)^2} - \left(\frac{\omega_P}{\omega}\right)^2 \epsilon_\infty \quad (2)$$

and the plasma frequency, ω_P , is given by

$$\omega_P^2 = \frac{4\pi Ne^2}{m^* \epsilon_\infty} \quad (3)$$

In these equations $\epsilon_\infty = 5.2$ is the high frequency dielectric constant obtained from the zero wavelength intercept (16%) of Piper and Marple's reflectivity data⁽¹⁾ using

$$\epsilon_\infty = \left[\frac{1 + (R_\infty)^{1/2}}{1 - (R_\infty)^{1/2}} \right]^2 \quad (4)$$

$\epsilon_0 = 9.0$ ⁽⁶⁾ is the damped dielectric constant, $m^* = 0.20 m$ ^{(7), (8)} is the effective

electron mass, n is the density of carriers, e is the electron charge, and $\omega_t = 4.56 \times 10^{13} \text{ sec}^{-1}$ is the transverse optical phonon frequency.⁽⁹⁾ $\epsilon_T(0, \omega)$ is the total dielectric constant.

The Varga theory as such has been verified by Mooradian and Wright⁽¹⁰⁾ from Raman spectra in GaAs. As far as reflectivity data are concerned the free-electron damping has a strong influence on reducing the reflectivity from the "square" undamped results found by Varga.⁽²⁾ The two minimum reflection regions found by Singwi and Tosi and Varga are partially filled and the peaks become skewed. However, Singwi and Tosi⁽¹⁰⁾ still indicate a result that shows a region near the phonon resonance frequency in which the reflectivity is one hundred percent. This is unrealistic because, as they point out, phonon damping is neglected in their calculation.

The reflectivity can be reduced from one hundred percent when phonon and electron damping are included in the phonon-plasmon interaction. Assuming that dielectric constants are additive,⁽¹⁰⁾ one may write a total dielectric constant, ϵ_T , as

$$\epsilon_T = \epsilon_\infty + \epsilon_{DL} + \epsilon_{DE} \quad (5)$$

where ϵ_∞ is the high frequency dielectric constant

$$\epsilon_{DL} = \frac{(\epsilon_0 - \epsilon_\infty) \left[1 - \left(\frac{\omega}{\omega_t} \right)^2 \right]}{\left[1 - \left(\frac{\omega}{\omega_t} \right)^2 \right]^2 + \left(\frac{\Gamma}{\omega_t} \right)^2 \left(\frac{\omega}{\omega_t} \right)^2} + i \frac{(\epsilon_0 - \epsilon_\infty) \left(\frac{\omega}{\omega_t} \right) \left(\frac{\Gamma}{\omega_t} \right)}{\left[1 - \left(\frac{\omega}{\omega_t} \right)^2 \right]^2 + \left(\frac{\Gamma}{\omega_t} \right)^2 \left(\frac{\omega}{\omega_t} \right)^2} \quad (6)$$

is the complex dielectric constant representing the damped harmonic oscillator, ⁽¹¹⁾

$$\epsilon_{DE} = - \frac{\omega_P^2 \epsilon_\infty}{\omega^2 + \frac{\Gamma^2}{\tau^2}} + i \frac{\omega_P^2 \frac{\epsilon_\infty}{\tau}}{\omega^2 + \frac{\Gamma^2}{\tau^2}} \quad (7)$$

is the damped free electron or plasmon term as given by Pines. ⁽¹²⁾ In these expressions, ω is the frequency of the radiation, Γ is the damping factor for the phonons and, τ is the free carrier damping term expressed as a lifetime.

In practice one would determine Γ , ω_t , ϵ_0 , and ϵ_∞ from a fit of the reflectivity data from a sample with very low carrier concentration. (For CdS, $\Gamma = 7.74 \text{ cm}^{-1}$ ⁽⁵⁾.) Then one would compare theory and experiment with doped samples to determine τ .

With

$$\epsilon_T = (n^2 - K^2) + i(2nK) \quad (8)$$

and the reflectivity, R , given by

$$R = \frac{(n-1)^2 + K^2}{(n+1)^2 + K^2} \quad (9)$$

where n is the index of refraction and K is the extinction index, one can use this dispersion fit to obtain τ . This reflectivity will differ from the Singwi and Tosi case in that it will result in the more realistic case where reflectivity peaks do not reach one hundred percent and appear even more skewed. The result of two reflectivity minimums will still remain with not too small a value

for τ .

Figures 2 and 3 show this procedure applied to the data of Piper and Marple. However, τ is set equal to ∞ since not enough data are available for a curve fit.

Reflectivity data available from doped samples of Mg_2Sn ⁽¹³⁾ suggest that a second minima may be found from the curve fitting done at shorter wavelengths using the dielectric function of Varga but with phonon damping and finite plasmon lifetime. Complete reflection data and analysis are given for $ZnTe$ ⁽¹⁴⁾ where finite lifetimes are used for the plasma oscillations of both light and heavy holes. The minima are washed out in $ZnTe$ because of the extreme damping.

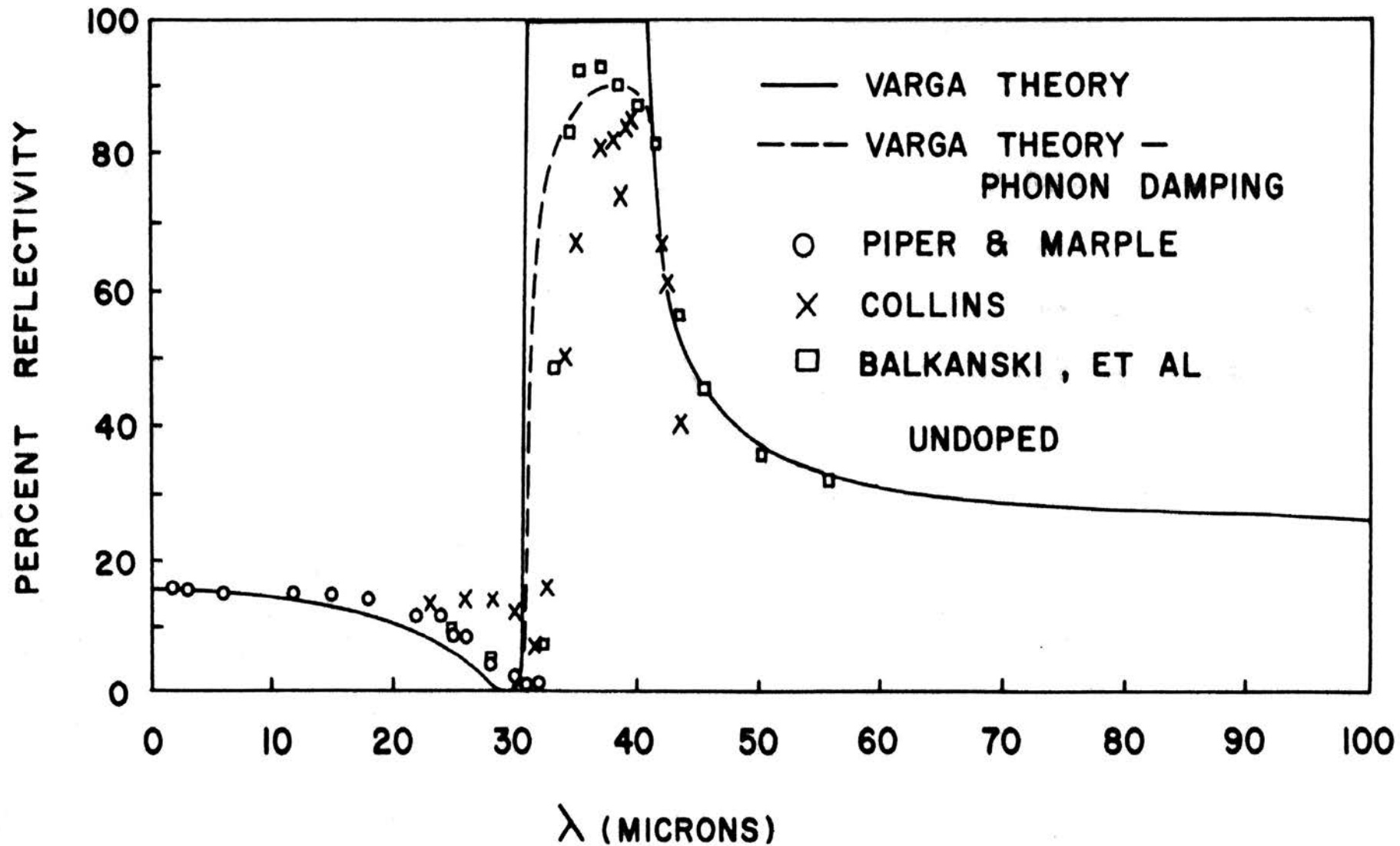


Figure 1: Percent reflectivity vs wavelength for undoped CdS.

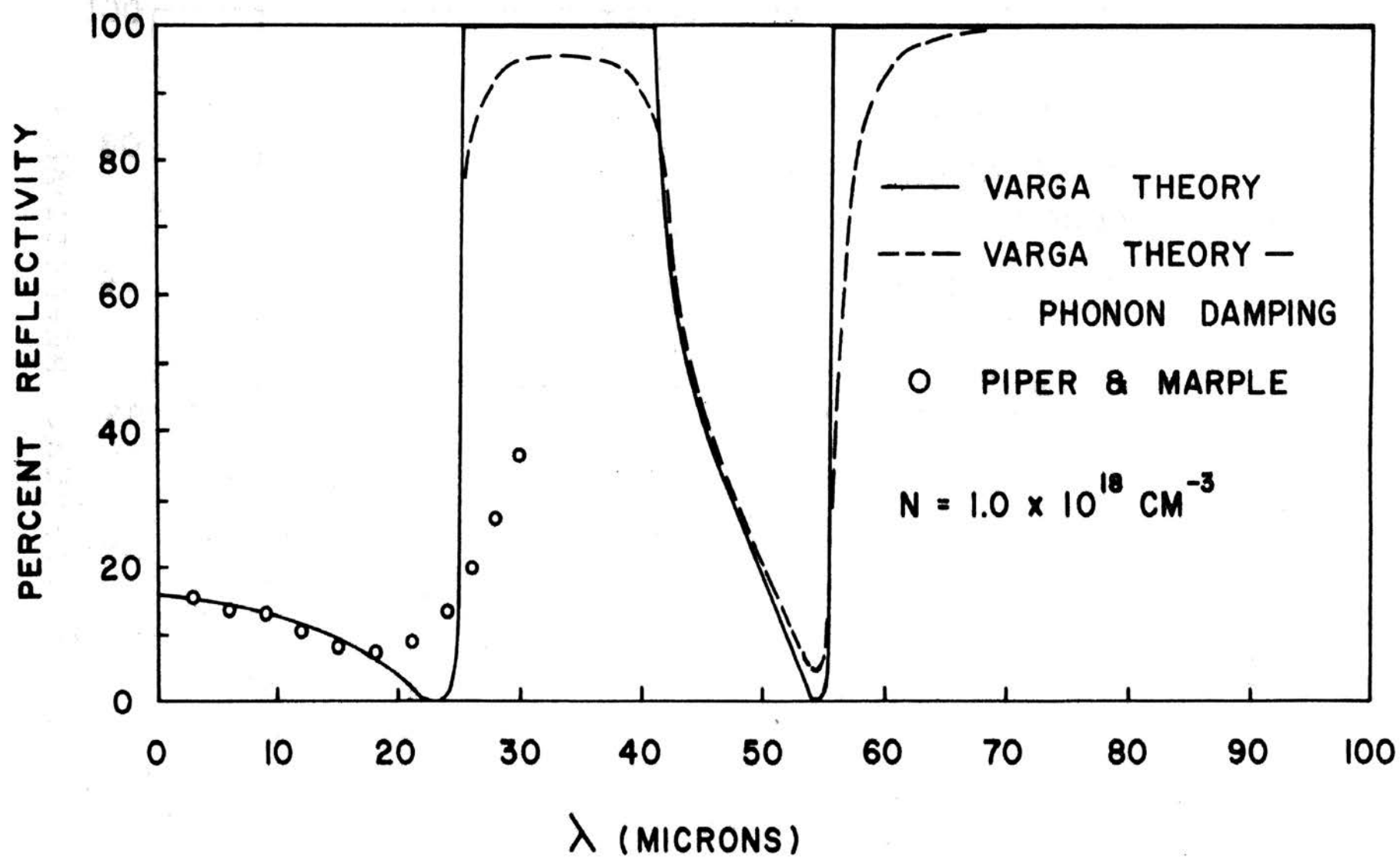


Figure 2: Percent reflectivity vs wavelength for Ga-doped CdS. $N=1.0 \times 10^{18} \text{ cm}^{-3}$.

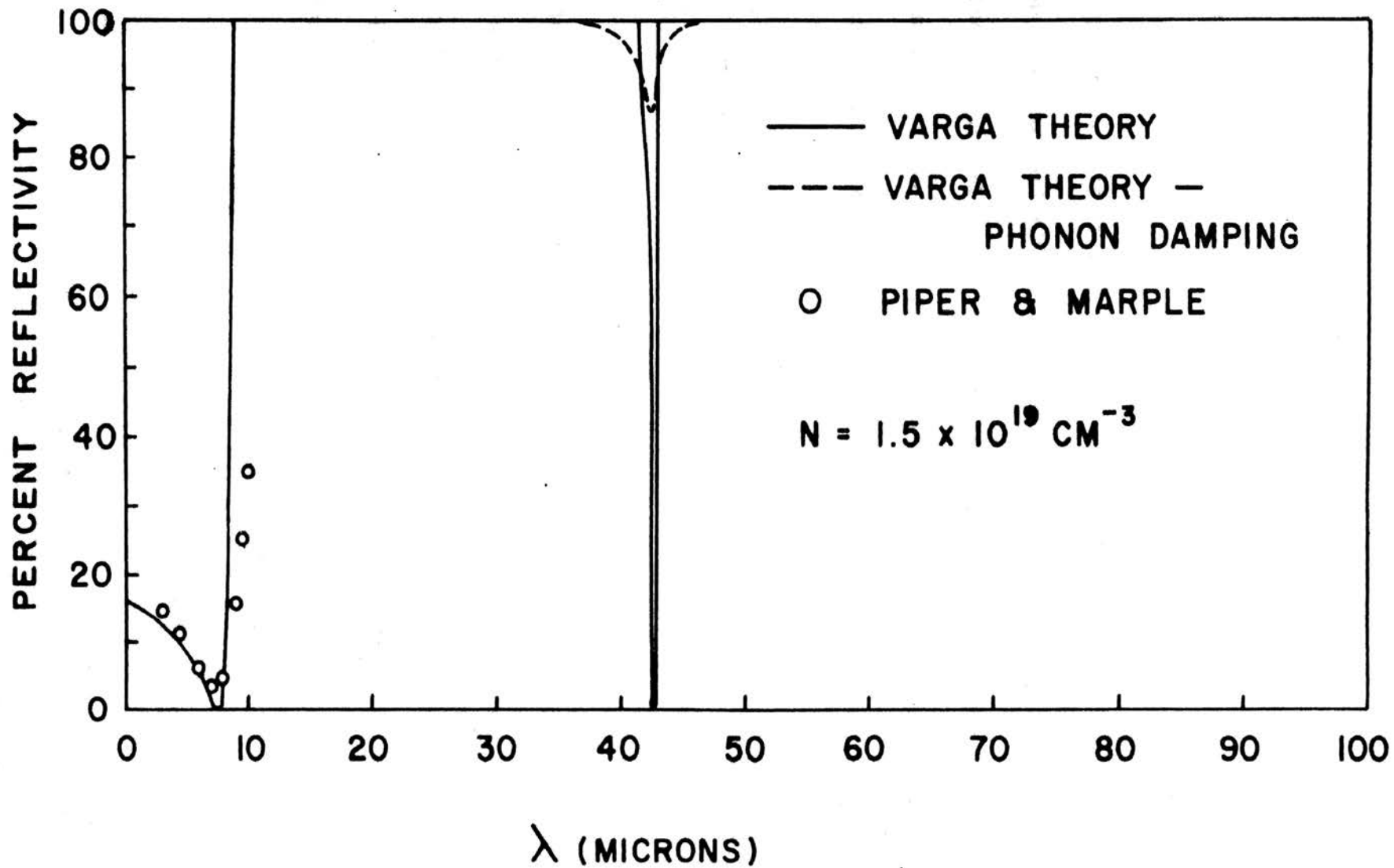


Figure 3: Percent reflectivity vs wavelength for Ga-doped CdS. $N=1.5 \times 10^{19} \text{ cm}^{-3}$.

III. REFLECTIVITY MINIMA

In a previous publication⁽¹⁶⁾ the reflectivity minimum wavelength was studied from the viewpoint of Murry, et. al.⁽¹⁷⁾, who treated the dielectric constant as the sum of a frequency independent lattice term and a frequency dependent plasmon term. This necessarily fails when the plasma frequency approaches the longitudinal optic frequency, since no such terms appear.

Their results in CdS are plotted as a dashed line in Figure 4 using $\epsilon_\infty = 5.2$ ⁽¹⁾ instead of 4.6 as used in publication⁽¹⁶⁾ based on Collins data⁽⁴⁾. The short and long wave length minima predicted by Varga may be shown to be

$$\omega_{\min}^2 = \frac{\epsilon_0 \left(1 + \left(\frac{\omega_P}{\omega_1}\right)^2\right) - 1 \pm \left[\left(\left[\epsilon_0 \left(1 + \left(\frac{\omega_P}{\omega_1}\right)^2\right) - 1 \right]^2 - 4 \left(\frac{\omega_P}{\omega_1}\right)^2 \epsilon_0 (\epsilon_\infty - 1) \right)^{1/2} \right]}{2 \left(\frac{\epsilon_\infty - 1}{\omega_t} \right)} \quad (10)$$

where the short wavelength (+ sign) is more valid than the long wavelength (- sign) since the extinction index K has been assumed zero. These wavelength minima have been plotted as Varga's Theory (using the Lyddane-Sachs-Teller relation) in figure 4 and the circles from the data of Piper and Marple⁽¹⁾ show quite good agreement even as $\omega_P \rightarrow \omega_1$ at low concentration.

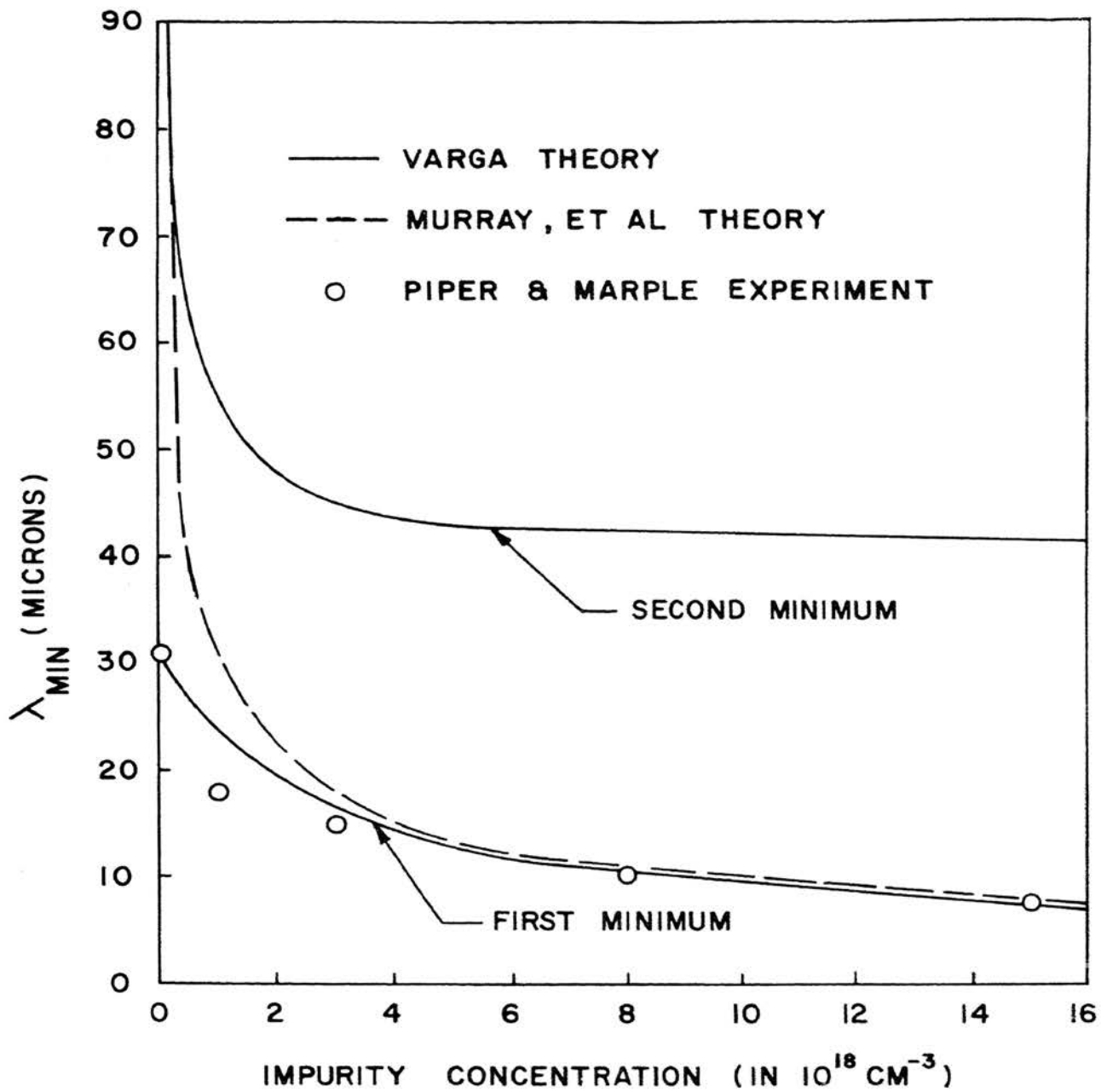


Figure 4: Wavelength at reflectivity minimum vs impurity concentration for Ga-doped CdS.

IV. DISCUSSION

The fact that the Varga theory has predicted so well the reflection minima versus impurity concentration in CdS, particularly at smaller levels, should be investigated further since the required condition for a degenerate electron gas obviously fails. Note that the degeneracy ratio, r_s , from Varga is given by⁽²⁾

$$r_s = \frac{d_{e-e}}{a'_0} \approx \frac{10^{-6} \text{ cm}}{a'_0 \epsilon_\infty m/m^*} \approx 8 \quad (11)$$

where the distance between carrier electrons, d_{e-e} , divided by the effective Bohr radius, a'_0 , is not less than 1 at concentrations of $10^{18}/\text{cc}$. For cases where r_s is less than 1, the self consistent field theory⁽¹⁸⁾ is applicable and the polarizabilities of the electrons and ions may be taken as additive. Varga's results are then derived for $r_s \ll 1$ from the equations of motion of Born and Huang⁽¹⁹⁾ and the Poisson equation.

REFERENCES

- (1) W. W. Piper and D. T. F. Marple, *J. Appl. Phys. Supplement to Vol 32*, 2237 (1961).
- (2) B. B. Varga, *Phys. Rev.* 137, 1135 (1965).
- (3) M. Born and K. Huang, *The Dynamical Theory of Crystal Lattices* (Clarendon Press, Oxford, 1956). 1st ed., p. 99.
- (4) R. J. Collins, *J. Appl. Phys.* 30, 1135 (1959).
- (5) M. Balkanski, M. Nusimovici, and R. Le Toullec, *J. de Physique*, 25, 305 (1964).
- (6) D. Berlincourt, H. Jaffe, and L. R. Shiozawa, *Phys. Rev.* 129, 1009 (1963).
- (7) A. Misu, K. Aoyagi, G. Kuwabara, and S. Sugano, *Internatl. Conf. on Semicond., Paris* (Acad. Press Inc., N. Y. 1964). p. 317.
- (8) J. J. Hopfield and D. G. Thomas, *Phys. Rev.* 119, 570 (1960).
- (9) M. Balkanski, J. M. Besson, and R. Le Toullec, *Internatl. Conf. on Semicond., Paris* (Academic Press, Inc., N. Y. 1964). p. 1091.
- (10) K. S. Singwi and M. P. Tosi, *Phys. Rev.* 147, 658 (1966).
- (11) A. Morradian and G. B. Wright, *Phys. Rev. Let.* 16, 999 (1966).
- (12) D. Pines, *Elementary Excitations in Solids* (W. A. Benjamin, Inc., New York, 1963), p. 208.
- (13) Herbert G. Lipson and Alfred Kahah, *Phys. Rev.* 158, 756 (1967).
- (14) R. J. Collins and D. A. Kleinman, *J. Phys. Chem. Solids*, 11, 190 (1959).
- (15) S. Narita, H. Harada, K. Nagasaka, *J. Phys. Soc. of Japan*, 22, 1176 (1967).
- (16) Robert J. Bell, "Plasma Coupling in CdS", *Phys. Let.* 24A, 576 (1967).
- (17) L. A. Murray, J. J. Rivera, and P. A. Hass, *J. Appl. Phys.* 37, 4743 (1966).
- (18) J. Lindhard, *Kgl. Danske Videnskab, Selskab, Mat. - fys. Medd.* 28, 8 (1954).
- (19) M. Born and K. Huang, *The Dynamical Theory of Crystal Lattices* (Clarendon Press, Oxford, 1956). 1st ed., p. 82.

SECTION D

Transmittance of Cer-Vit Glass-Ceramic
in the Ultraviolet, Visible, Infrared
and Submillimeter Wavelength Regions⁺

R. M. Fuller^{*}

D. G. Rathbun

Physics Department

University of Missouri at Rolla

Rolla, Missouri

Robert J. Bell

Physics Department and

Materials Research Center

University of Missouri at Rolla

Rolla, Missouri

⁺Work partially supported by National Science Foundation

^{*}On leave from Alma College, Alma, Michigan

Recently, Owens-Illinois⁽¹⁾ introduced a new family of materials under the trade name "Cer-Vit" which has a coefficient of thermal expansion of less than 10^{-7} per degree centigrade. This material may be ideal for optical parts when extremely low thermal expansion is required, and it is presently being used in a telescope at the University of Toledo⁽²⁾ and has been selected for use at several other installations.

This letter gives the transmittance of "Cer-Vit" material, type C-101, between 0.1920 and 1200 micrometers and the index of refraction between 200 and 1200 micrometers. Measurements were made on 1.125 ± 0.005 and 0.290 ± 0.005 mm thick samples of this material between 0.1920 and 2.7 micrometers with a Perkin-Elmer 450 spectrophotometer and between 2.5 and 50 micrometers with a Beckman IR-12 spectrophotometer. These data are given in Figure 1. The transmittances of 0.290 ± 0.005 and 0.49 ± 0.02 mm thick samples were measured on a vacuum submillimeter spectrometer. This is a single beam, $f/2.2$, echelette grating instrument covering the range of 40 to 1200 micrometers wavelength with a resolving power of about 100 to 200 using a Golay cell detector. Its source and output are similar to those of Russell and Strauss⁽³⁾, its chopper is similar to that of Bell and Gilmer⁽⁴⁾, its monochromator is similar to that of Richards⁽⁵⁾, and its filtering is as by Bell, et al⁽⁶⁾. These data are shown in Figure 2. No transmission was observed between 6.5 and 200 micrometers. The gap between 420 to 500 micrometers is due to poor grating overlap where the transmitted intensity was too low to obtain meaningful results. This is indicated by a single averaged datum point with appropriate error bars.

Note that the channel spectra were observed in the 200 to 1200 micrometer range enabling the index of refraction to be calculated from the relation⁽⁷⁾

$$m = \frac{2 n d}{\lambda} \cos \phi$$

where m = order number, n = index of refraction, d = sample thickness, ϕ = angle of refraction, and λ = wavelength. Since the angle of refraction was calculated to be less than 4 degrees, $\cos \phi$ was taken as 1. The values of index of refraction using the first 5 order peaks of the 0.29 mm thick sample are given in Table 1.

It is to be noted that smoothing out the transmittance data results in a transmittance curve similar to that of other glassy materials as obtained by McCubbin and Sinton⁽⁸⁾ and Dianov, et al⁽⁹⁾.

The authors wish to thank Miss B. Brooks[#] for assisting in the sample preparation, and Mr. J. Blea for assistance in obtaining data.

[#]NSF Undergraduate Research Trainee

TABLE 1

Index of refraction		
Order number	Wavelength (Micrometers)	Index of refraction
1	1160	2.0
2	630	2.2
3	440	2.3
4	340	2.3
5	265	2.3

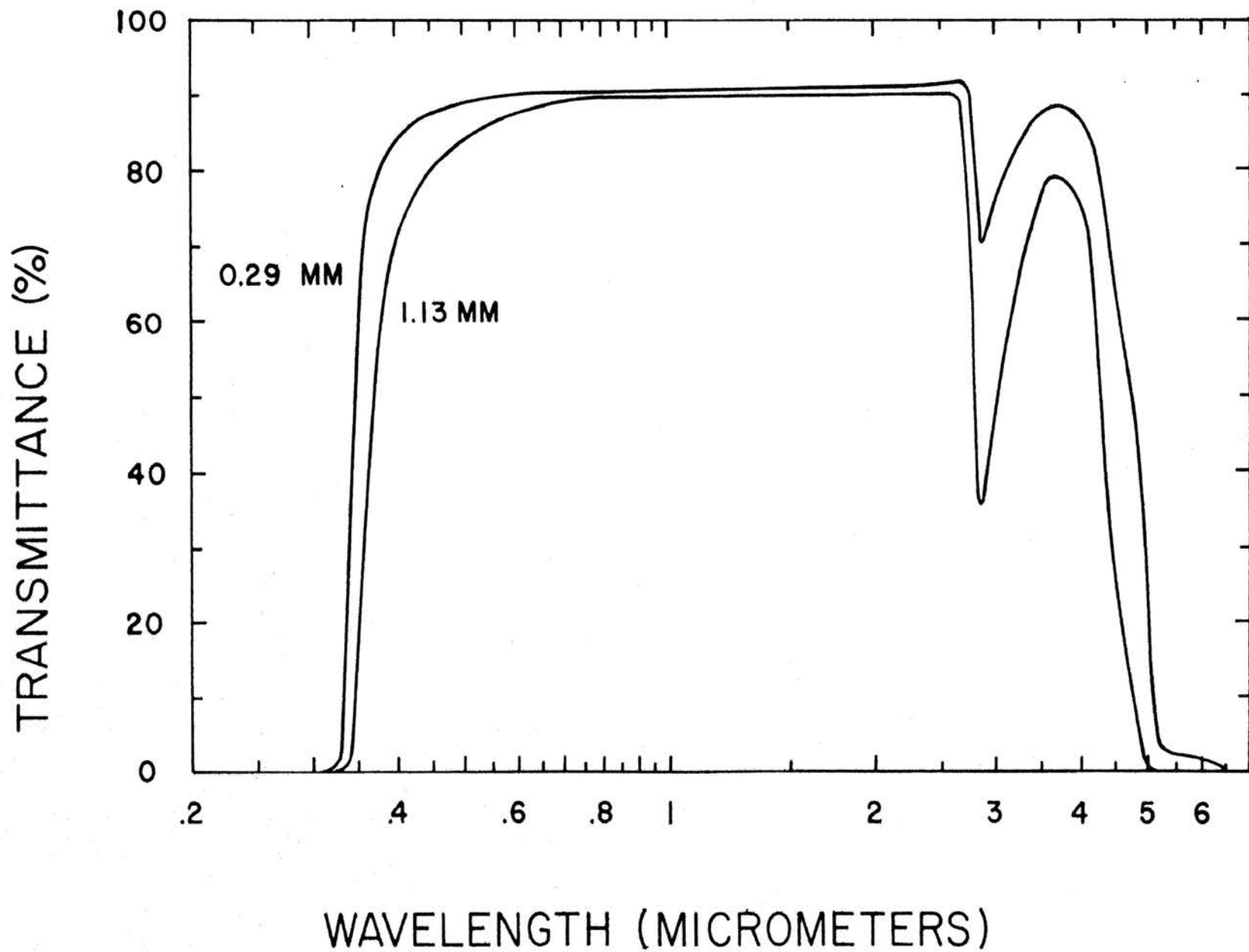


Figure 1: Transmittance of Cer-Vit Glass-Ceramic in the ultraviolet, visible, and infrared wavelength regions.

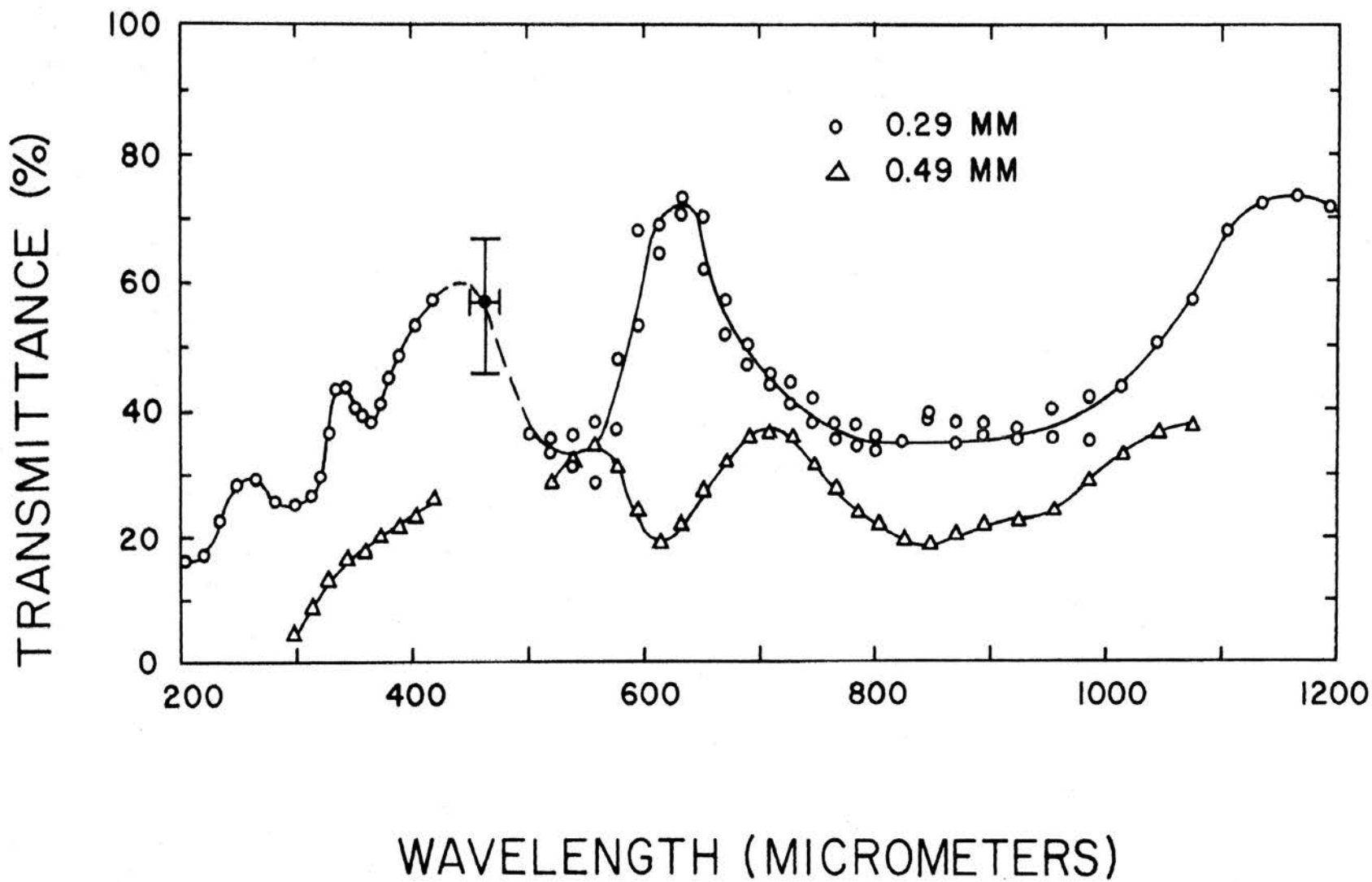


Figure 2: Transmittance of Cer-Vit Glass-Ceramic in the submillimeter wavelength region.

REFERENCES

- (1) Owens-Illinois, Toledo, Ohio.
- (2) Physics Today 21, (2), 55 (1968).
- (3) J. W. Russell and H. L. Strauss, Appl. Optics 4, 1131 (1965).
- (4) R. J. Bell and T. E. Gilmer, Jr., Appl. Optics 4, 45 (1965).
- (5) P. L. Richards, J. Opt. Soc. Am. 54, 1474 (1964).
- (6) R. J. Bell, S. I. Drasky, and W. L. Barnes, Infrared Physics 7, 57 (1967).
- (7) J. Strong, Concepts of Classical Optics, (W. H. Freeman and Co., San Francisco, Calif., 1958) p. 232.
- (8) T. K. McCubbin, Jr. and W. M. Sinton, J. Opt. Soc. Am. 40, 537 (1950).
- (9) E. M. Dianov, N. A. Irisova, V. N. Timofeev, Soviet Physics-Solid State, 8, 2113 (1967).

VITA

The author was born on March 20, 1935 at Whitehall, New York. He received his primary education in Whitehall, New York and Cheektowaga, New York and his secondary education in Whitehall, New York where he was graduated in June, 1952.

He was employed by General Electric Company in Schenectady, New York as an apprentice draftsman from April, 1953 until June, 1957, at which time he was inducted into military service. Following his separation from the military in June, 1959, he rejoined General Electric Company in Cincinnati, Ohio as a detail draftsman where he remained until May, 1962. From that time until September, 1963 he was employed as a design draftsman at McDonnell Aircraft Corporation in St. Louis, Missouri.

In September, 1963 he enrolled at the University of Missouri at Rolla and received a Bachelor of Science Degree in Physics in May, 1967. Since that time he has been enrolled in the Graduate School of the University of Missouri at Rolla as a research assistant.

132947